J|A|C|S
ARTICLES
Published on Web 02/18/2006

Rapid Purification and Size Separation of Gold Nanoparticles via Diafiltration

Scott F. Sweeney, Gerd H. Woehrle,† and James E. Hutchison*

Contribution from the Department of Chemistry and Materials Science Institute, University of Oregon, Eugene, Oregon, 97403

Received August 24, 2005; E-mail: hutch@uoregon.edu

Abstract: Purification and size-based separation of nanoparticles remain significant challenges in the preparation of well-defined materials for fundamental studies and applications. Diafiltration shows considerable potential for the efficient and convenient purification and size separation of water-soluble nanoparticles, allowing for the removal of small-molecule impurities and for the isolation of small nanoparticles from larger nanostructures in a single process. Herein, we report studies aimed at assessing the suitability of diafiltration for (i) the purification of water-soluble thiol-stabilized 3-nm gold nanoparticles, (ii) the separation of a bimodal distribution of nanoparticles into the corresponding fractions, and (iii) the separation of a polydisperse sample into fractions of differing mean core diameter. NMR, thermogravimetric analysis (TGA), and X-ray photoelectron spectroscopy (XPS) measurements demonstrate that diafiltration produces nanoparticles with a much higher degree of purity than is possible by dialysis or a combination of solvent washes, chromatography, and ultracentrifugation. UV−visible spectroscopic and transmission electron microscopic (TEM) analyses show that diafiltration offers the ability to separate nanoparticles of disparate core size. These results demonstrate the applicability of diafiltration for the rapid and green preparation of high-purity gold nanoparticle samples and the size separation of heterogeneous nanoparticle samples. They also suggest the development of novel diafiltration membranes specifically suited to high-resolution nanoparticle size separation.

I. Introduction

Development of methods that provide convenient access to ligand-stabilized nanoparticles, offer greater control of structural definition, and can be conducted at larger scales is becoming increasingly important for fundamental studies[1−5] and applications[6−13] of nanoparticles. In particular, a high degree of purity and monodispersity are often crucial as these variables can complicate the assessment of structure−function relationships, confound electronic and optical measurements, or impede the self-assembly processes by which nanoscaled structures are prepared.[14,15] Although a number of syntheses of gold nanoparticles have been developed that allow for the preparation of nanoparticles of varying core dimension and surface functionality,[16−22] a significant challenge remains in developing strategies for the preparation of nanoparticles of high purity (i.e., free of excess ligand, salt, and starting material) and that exhibit low polydispersity. An additional challenge remains in the removal of nanoparticle monomers and aggregates from well-defined self-assembled nanoparticle superstructures.[23,24]

The influence of purity on the chemistry and properties of nanoparticles is often overlooked; however, recent results indicate that the extent of purification can have a significant impact. Kalyuzhny and Murray[25] have recently reported the effects of purification on the optical properties of CdSe

† Present address: Abbott GmbH & Co. KG, Soliqs Drug Delivery Business, Knollstr. 50, 60761 Ludwigshafen, Germany.

(1) Peng, Z. Q.; Walther, T.; Kleinermanns, K. *Langmuir* **2005**, *21*, 4249−4253.
(2) Lim, I. I. S.; Maye, M. M.; Luo, J.; Zhong, C. J. *J. Phys. Chem B* **2005**, *109*, 2578−2583.
(3) Wei, Z. Q.; Zamborini, F. P. *Langmuir* **2004**, *20*, 11301−11304.
(4) Goodman, C. A.; Frankamp, B. L.; Cooper, B. A.; Rotello, V. A. *Colloids Surf. B: Biointerfaces* **2004**, *39*, 119−123.
(5) Alivisatos, A. P. *J. Phys. Chem.* **1996**, *100*, 13226−13239.
(6) Bartz, M.; Kuther, J.; Seshadri, R.; Tremel, W. *Angew. Chem., Int. Ed.* **1998**, *37*, 2466.
(7) Boal, A. K.; Rotello, V. M. *J. Am. Chem. Soc.* **2000**, *122*, 734−735.
(8) Frey, P. A.; Frey, T. G. *J. Struct. Biol.* **1999**, *127*, 94−100.
(9) Hainfeld, J. F. *Science* **1987**, *236*, 450−453.
(10) Huang, D.; Liao, F.; Molesa, S.; Redinger, D.; Subramanian, V. *J. Electrochem. Soc.* **2003**, *157* (7), 412−417.
(11) Jahn, W. *J. Struct. Biol.* **1999**, *127*, 106−112.
(12) Neiman, B.; Grushka, E.; Lev, O. *Anal. Chem.* **2001**, *73*, 5220−5227.
(13) Wohltjen, H.; Snow, A. W. *Anal. Chem.* **1998**, *70*, 2856−2859.
(14) Kearns, G. J.; Foster, E. W.; Hutchison, J. E. *Anal. Chem.* **2006**, *78*, 298−303.
(15) Foster, E. W.; Kearns, G. J.; Goto, S.; Hutchison, J. E. *Adv. Mater.* **2005**, *17*, 1542−1545.
(16) Brust, M.; Bethell, D.; Schiffrin, D. J.; Kiely, C. J. *Adv. Mater.* **1995**, *7*, 795−797.
(17) Brust, M.; Fink, J.; Bethell, D.; Schiffrin, D. J.; Kiely, C. J. *J. Chem Soc., Chem. Commun.* **1995**, *6*, 1655−1656.
(18) Foos, E. E.; Snow, A. W.; Twigg, M. E.; Ancona, M. G. *Chem. Mater.* **2002**, *14*, 2401−2408.
(19) Hostetler, M. J.; Wingate, J. E.; Zhong, C.-J.; Harris, J. E.; Vachet, R. W.; Clark, M. R.; Londono, J. D.; Green, S. J.; Stokes, J. J.; Wignall, G. D.; Glish, G. L.; Porter, M. D.; Evans, N. D.; Murray, R. W. *Langmuir* **1998**, *14*, 17−30.
(20) Kanaras, A. G.; Kamounah, F. S.; Schaumburg, K.; Kiely, C. J.; Brust, M. *J. Chem Soc., Chem. Commun.* **2002**, 2294−2295.
(21) Weare, W. W.; Reed, S. M.; Warner, M. G.; Hutchison, J. E. *J. Am. Chem. Soc.* **2000**, *122*, 12890−12891.
(22) Yonezawa, T.; Sutoh, M.; Kunitake, T. *Chem. Lett.* **1997**, 619−620.
(23) Cumberland, S. L.; Berrettini, M. G.; Javier, A.; Strouse, G. F. *Chem. Mater.* **2003**, *15*, 1047−1056.
(24) Wang, D.; Jibao, H.; Rosenzweig, N.; Rosenzweig, Z. *Nano Lett.* **2004**, *4*(3), 409−413.
(25) Kalyuzhny, G.; Murray, R. W. *J. Phys. Chem B* **2005**, *109*, 7012−7021.

10.1021/ja0558241 CCC: $33.50

nanoparticles showing that PL intensity and peak location changes with differing concentration of free ligand in solution. Ploehn and co-workers[26] have reported that the extent of purification of dendrimer-encapsulated Pt nanoparticles can bias size determination via atomic force microscopy (AFM). We have recently shown that the self-assembly of gold nanoparticles in 1D and 2D arrays is dependent upon the purity of the gold nanoparticles.[14,15] It is also known that gold nanoparticles in the presence of excess thiol ligand (as with ligand exchange) will rapidly decompose.[27] These results underscore the necessity of identifying convenient, efficient, and more stringent purification methods for nanoparticle samples.

The purification of water-soluble gold nanoparticles is particularly difficult because the nanoparticles and the impurities have similar solubility, often making standard purification techniques (i.e., precipitation, extraction, chromatography, centrifugation, or dialysis) inadequate or inefficient.[16,20,21,28] Although reasonable purity is afforded via these methods, the nanoparticles remain contaminated with precursor molecules, for example, salts and free ligand. In addition, conventional purification methods do not address several significant challenges, namely, large volumes of organic waste, the high cost of chromatography supports, time intensiveness, and the ability to reasonably prepare large quantities of nanoparticles. Finally, most purification schemes are developed for one type of nanoparticle and are often not applicable for the purification of nanoparticles with differing core or ligand shell properties.

Similar, but often more challenging, issues are faced in approaches for decreasing the polydispersity of nanoparticle samples. Particle size and size dispersity can be controlled to a certain extent by synthetic methods, such as deliberate variation of the gold-to-ligand ratio[19] and dendrimer encapsulation;[29−31] however, these methods are often sensitive to minute changes in reaction conditions. Centrifugation,[32] electrophoresis,[33,34] fractional crystallization,[35] chromatography,[32,36−38] stirred-cell ultrafiltration,[39] and size-dependent solubility[35,40] have been reported for size-based separation. Unfortunately, the fractionation of nanoparticle samples by these methods is often dependent upon specific core or ligand shell properties, time-consuming, difficult, and expensive.

Diafiltration offers a versatile alternative to the methods described above for the purification and size separation of nanoscale materials. Though not yet reported for the preparation of water-soluble gold nanoparticles, diafiltration has been used frequently for biological[41,42] and colloidal applications.[43,44] Diafiltration is a membrane-based method wherein pore size dictates the retention and elution of material from a sample, as depicted in Figure 1. This approach offers the opportunity to consolidate purification and size separation into a single step, making diafiltration more efficient than any combination of previously reported techniques. Due to simple equipment requirements and the scalability[45] of the technique, diafiltration is affordable, convenient, and versatile. Furthermore, the membranes can be reused and organic solvent dependence is reduced, contributing to greener nanoparticle syntheses.[46,47]

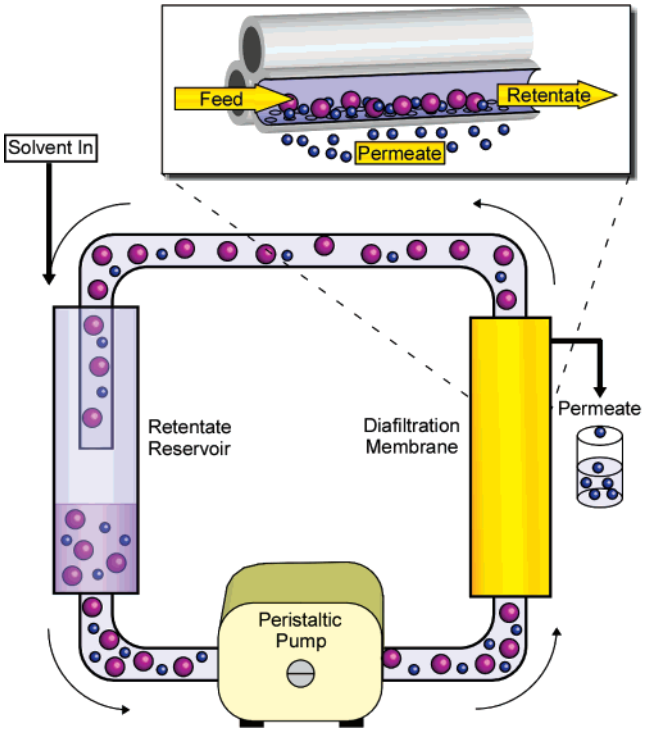

Figure 1. Schematic of the continuous diafiltration setup used in this study. Sample and makeup solution are introduced to the retentate reservoir. The solution is pumped by the peristaltic pump through the diafiltration membrane. Small molecule impurities or small nanoparticles (blue) are eluted in the permeate, while the large nanoparticles (purple) are retained. The expanded view is of a hollow-fiber-type diafiltration membrane and depicts the elution of small impurities and nanoparticles and the retention of larger particles.

In this article, we report that diafiltration is a rapid and convenient approach to the preparation of higher purity water-soluble gold nanoparticles and has considerable potential as a method for the size separation of heterogeneous nanoparticle samples. We compare diafiltration to conventional purification

(26) Xie, H.; Gu, Y. L.; Ploehn, H. J. *Nanotechnology* **2005**, *16*, S492−S501.
(27) (a) Woehrle, G. H.; Brown, L. O.; Hutchison, J. E. *J. Am. Chem. Soc.* **2005**, *127*, 2172−2183. (b) Woehrle, G. H.; Warner, M. G.; Hutchison, J. E. *Langmuir* **2004**, *20*, 5982−5888.
(28) Brust, M.; Walker, M.; Bethell, D.; Schiffrin, D. J.; Whyman, R. J. *J. Chem Soc., Chem. Commun.* **1994**, *5*, 801−802.
(29) Sang-Keun, O.; Kim, Y.; Ye, H.; Crooks, R. M. *Langmuir* **2003**, *19*, 10420−10425.
(30) Kim, Y.; Sang-Keun, O.; Crooks, R. M. *Chem. Mater.* **2004**, *16*, 167−172.
(31) Crooks, R. M.; Zhao, M.; Sun, L.; Chechik, V.; Yeung, L. K. *Acc. Chem. Res.* **2001**, *34* (3), 181−190.
(32) Novak, J. P.; Nickerson, C.; Franzen, S.; Feldheim, D. L. *Anal. Chem.* **2001**, *73*, 5758−5761.
(33) Smith, J. *Bull. Kor. Chem Soc.* **2003**, *24*, 684−686.
(34) Templeton, A. C.; Cliffel, D. E.; Murray, R. W. *J. Am. Chem. Soc.* **1999**, *121*, 7081−7089.
(35) Chemseddine, A.; Weller, H. *Ber. Bunsen-Ges. Phys. Chem.* **1993**, *97*, 636.
(36) Al-Somali, A. M.; Krueger, K. M.; Falkner, J. C.; Colvin, V. L. *Anal. Chem.* **2004**, *76*, 5903−5910.
(37) Krueger, K. M.; Al-Somali, A. M.; Falkner, J. C.; Colvin, V. L. *Anal. Chem.* **2005**.
(38) Song, Y.; Heien, M. L.; Jimenez, V.; Wightman, R. M.; Murray, R. W. *Anal. Chem.* **2004**, *76*, 4911−4919.
(39) Akthakul, A.; Hochbaum, A. I.; Stellacci, F.; Mayes, A. M. *Adv. Mater.* **2005**, *17*, 532−535.
(40) Clarke, N. Z.; Waters, C.; Johnson, K. A.; Satherly, J.; Schiffrin, D. J. *Langmuir* **2001**, *17*, 6048−6050.
(41) Ebersold, M. F.; Zydney, A. L. *Biotechnol. Prog.* **2004**, *20*, 543−549.
(42) Lajmi, A. R.; Schwartz, L.; Sanghvi, Y. S. *Org. Process Res. Dev.* **2004**, *8*, 651−657.
(43) Tishchenko, G.; Luetzow, K.; Schauer, J.; Albrecht, W.; Bleha, M. *Sep. Purif. Technol.* **2001**, *22−23*, 403−415.
(44) Limayem, I.; Charcosset, C.; Fessi, H. *Sep. Purif. Technol.* **2004**, *38*, 1−9.
(45) Although we focus on small quantities of material (∼100 mg), diafiltration allows for purification of kilogram-scale quantities of material. This is important because as the preparation of nanoparticles is scaled, the same purification procedure can be used, allowing for consistent preparation at all scales.
(46) McKenzie, L. C.; Hutchison, J. E. *Chim. Oggi-Chem. Today* **2004**, *22*, 30−33.
(47) Anastas, P. T.; Warner, J. C. *Green Chemistry Theory and Practice*; Oxford University Press: Oxford, U.K., 1998.

methods, demonstrating through XPS, TGA, and ^{1}H NMR analyses that diafiltration yields nanoparticles of higher purity, in less time (~15 min vs 3 days) and with less waste (4 L of H_2O/g of product vs 15 L of solvent/g of product) than conventional methods such as dialysis extractions, centrifugation, and chromatography. The size separation of a mixture of 1.5- and 3-nm nanoparticles is also presented, demonstrating through TEM and UV−vis analyses the utility of diafiltration for separating nanomaterials of disparate core dimensions. Finally, we report on the fractionation of a polydisperse 3-nm sample into four fractions of differing mean core diameter. Analysis of these fractions by UV−vis spectroscopy and TEM demonstrates the potential of diafiltration for fractionation and suggests areas of improvement in the pore morphology of diafiltration membranes. Our experiments demonstrate that diafiltration is an efficient and versatile approach for the consistent preparation of nanoparticle samples that exhibit a high degree of purity and that this method may prove useful for the size separation of nanoparticle samples.

II. Experimental Section

Materials. Hydrogen tetrachloroaurate ($HAuCl_4 \cdot 3H_2O$) was obtained from Strem Chemicals, Inc. and used as received. Nanopure water (18.2 MΩ·cm resistivity) was prepared with a Barnstead NANOpure filtration system and used for all aqueous samples. The thiol ligands 2-(2-mercaptoethoxy)ethanol (**1**) and 2-[2-(2-mercaptoethoxy)ethoxy]ethanol (**2**) were synthesized according to known procedures.[27] Sephadex LH-20 was obtained from GE Healthcare/Amersham Biosciences. Dialysis membranes (15 kDa; SpectraPor) were obtained from Spectrum. Poly(sulfone) diafiltration membranes (10, 30, 50, and 70 kDa; MiniMate) were obtained from Pall. All other reagents and solvents were purchased from Aldrich or Mallinckrodt and used as received.

Analytical Procedures. X-ray photoelectron spectroscopy (XPS) was performed on a Kratos HSi instrument operating at a base pressure of ~10^{-8} mmHg with monochromatic Al Kα radiation at 15 mA and 13.5 kV. Nanoparticles were drop-cast from concentrated aqueous solution onto a clean[48] silicon wafer. Samples were charge-compensated and binding energies were referenced to carbon 1s at 284.4 eV. UV−visible spectroscopy was performed on an Ocean Optics USB2000 spectrometer with 1 cm disposable plastic cuvettes. Thermogravimetric analysis (TGA) was performed on a Hi-Res TGA 2950 thermogravimetric analyzer. Lyophilized nanoparticle samples (3−5 mg) were placed into Al pans and heated at 10 °C/min to 110 °C, followed by a 10 min isotherm to remove any remaining solvent. The samples were then heated at 5 °C/min to 500 °C, followed by a 20 min isotherm to ensure no further mass loss. Nuclear magnetic resonance (NMR) spectra were collected at 25 °C on a Varian Unity Inova 300 MHz instrument. Transmission electron microscopy (TEM) was performed on a Phillips CM-12 microscope operating at 120 kV accelerating voltage. Aliquots of dilute nanoparticle samples (10 μL) were aerosoled onto SiO_x-coated 400-mesh copper TEM grids (Ted Pella) and dried under ambient conditions prior to inspection via TEM. Images were recorded and processed as described previously.[49,50]

General Diafiltration Procedure. The diafiltration setup used for the experiments reported herein is shown in Figure 1. Following preparation and dissolution in water, nanoparticle samples are transferred to the rententate reservoir (a 20 mL syringe with the plunger removed). The sample is drawn from the reservoir and into the diafiltration membrane through a peristaltic pump.[51] The speed of the pump is slowly increased to the maximum rate, equilibrating the feed pressure to the membrane at ~100 kPa. The rate of water addition to the reservoir is monitored and adjusted so that it equals the rate of elution. When the volume of material eluted is equal to the hold-up volume in the reservoir, this is considered one diafiltration volume. The diafiltration is continued through a number of volumes until the purification or size separation is complete. The relationship between the percent purity (% P) and the number of diafiltration volumes (V_D) is

$$\% P = (1 - e^{V_D(1-\sigma)}) \times 100 \quad (1)$$

where σ is the rejection coefficient, which is determined experimentally for different solutes and is affected by pore morphology, nanoparticle properties such as core diameter and surface functionality, and solution properties such as ionic strength. In the case of purification, σ is 0, meaning that five diafiltration volumes are necessary to see complete purification. In the case of size separation, 15 volumes ($\sigma = 0.33$) are often necessary.

Sample Descriptions. Samples for the purification experiment were prepared and stabilized with ligand **2**, and samples for the size separation experiments were prepared with ligand **1**. All diafiltered nanoparticle samples are named according to the convention Au_x-descriptor, where x is the mean core size of the particle and the descriptor defines the membrane pore size and whether the sample is the permeate or retentate. For example, $Au_{3.0}$-70R describes a 3.0-nm gold nanoparticle sample that is the retentate of a 70 kDa diafiltration. Exceptions to this scheme are crude nanoparticle samples, which are named Au_x-crude; samples purified via extraction, chromatography, and centrifugation, which are named Au_x-ECC; dialyzed samples, which are named Au_x-D; triphenylphosphine-stabilized particles, which are named Au_x-TPP; and the mixed 1.5- and 3-nm sample, which is named Au_x-mix.

Preparation of Water-Soluble ~3-nm Gold Nanoparticles ($Au_{\sim 3}$-Crude). Water-soluble 3-nm gold nanoparticles were synthesized by a procedure developed by Brust and co-workers[20] with minor modifications. Briefly, in a 100 mL round-bottom flask were dissolved **1** (0.0131 g, 0.107 mmol) or **2** (0.0178, 0.107 mmol) and $HAuCl_4$ (0.1094 g, 0.322 mmol) in 50 mL of 2-propanol, yielding a yellow solution. To this solution, 5 mL of a 3.5 M $NaBH_4$ solution in methanol was added rapidly with stirring, resulting in an immediate color change from yellow to dark purple. The solution was allowed to stir under ambient conditions for 2 h and then filtered through a 150 mL 60F fritted funnel. The resulting purple solid was collected from the frit and dissolved in 20 mL of water.

Water-Soluble ~3-nm Gold Nanoparticles Purified via Extraction, Chromatography, and Ultracentrifugation ($Au_{\sim 3}$-ECC). The water-soluble nanoparticles $Au_{\sim 3}$-crude (100 mg) were extracted with 5 × 20 mL of dichloromethane to remove excess ligand and disulfide. The aqueous layer was isolated and dried overnight under a stream of nitrogen. The resultant solid was dissolved in a minimum amount of water and purified via gel-permeation chromatography (Sephadex LH-20, eluent H_2O) to further remove salts and organic impurities. Following chromatography, the nanoparticles were centrifuged (and the supernatant removed) twice at 200 000 g for 10 h at 4 °C to remove any remaining impurities. The resultant nanoparticles were lyophilized and analyzed by XPS, NMR, TEM, and TGA.

Water-Soluble ~3-nm Gold Nanoparticles Purified via Dialysis ($Au_{\sim 3}$-D). The water-soluble nanoparticles $Au_{\sim 3}$-crude (50 mg) in 20 mL of water were transferred to a 15 kDa dialysis membrane and dialyzed with 3 × 3 L of water for 6 h each. Following dialysis, water was removed via rotary evaporation and the particles were resuspended

(48) Silicon wafers for XPS are cleaned by first sonicating the wafer in THF, followed by ethanol and water rinses. Next, the wafer is placed into 7:3 H_2SO_4/30% H_2O_2 and heated at 100 °C for 30 min. Finally, the wafer is cleaned in 200:4:1 H_2O/30% H_2O_2/NH_4OH.
(49) See Supporting Information.
(50) Woehrle, G. H.; Hutchison, J. E.; Ozkar, S.; Finke, R. G. *Turk. J. Chem.*, in press.
(51) For an initial evaluation of diafiltration, starter kits are available that utilize two syringes instead of a pump, allowing for manual purification by diafiltration.

in 10 mL of water. The resultant nanoparticles were lyophilized and analyzed via XPS, NMR, TEM, and TGA.

Water-Soluble ~3-nm Gold Nanoparticles Purified via Diafiltration ($Au_{\sim 3}$-70R). The water-soluble nanoparticles $Au_{\sim 3}$-crude (100 mg) were diafiltered with 5 × 20 mL of water with a 70 kDa diafiltration membrane. The solution was concentrated to 10 mL by ceasing makeup flow, and the nanoparticles were collected by pumping the solution into a 20 mL scintillation vial. The membrane was flushed with an additional 3−5 mL of water, which was combined with the original 10 mL. The resultant nanoparticles were lyophilized and analyzed by XPS, NMR, TEM, and TGA.

Synthesis of Triphenylphosphine-Stabilized 1.5-nm Nanoparticles ($Au_{1.5}$-TPP). Triphenylphosphine-stabilized nanoparticles, $Au_{101}(PPh_3)_{21}Cl_5$, were synthesized according to a previously described procedure.[21]

Water-Soluble 1.5-nm Gold Nanoparticles via Ligand Exchange ($Au_{1.5}$-10R).[27] $Au_{1.5}$-TPP (20 mg in 5 mL of CH_2Cl_2) and **1** (20 mg in 5 mL water) were stirred rapidly at room temperature for 6 h until the transfer of the darkly colored nanoparticles to the aqueous layer was complete. Upon completion of the exchange, the layers were separated and the residual CH_2Cl_2 was removed from the aqueous layer in vacuo. The aqueous layer was diafiltered with 5 × 10 mL of water with a 10 kDa diafiltration membrane.

Separation of 1.5- and 3.1-nm Water-Soluble Nanoparticles via Diafiltration. A mixture of $Au_{1.5}$-10R (3.9 mg) and $Au_{3.1}$-70R (39.1 mg) nanoparticles in 10 mL of water was diafiltered with 15 × 10 mL of water with a 50 kDa diafiltration membrane. At this point, the retentate ($Au_{2.9}$-50R) was collected as previously described and the combined permeate fractions were concentrated with a 10 kDa diafiltration membrane, yielding $Au_{1.5}$-50P. TEM images and UV−vis spectra were obtained for the initial nanoparticles and the nanoparticle mixture as well as for the permeate and retentate.

Fractional Separation of Water-Soluble 3-nm Gold Nanoparticles via Diafiltration. We prepared four nanoparticle fractions by performing a series of diafiltration steps using membranes of decreasing pore size. Following the preparation of $Au_{2.9}$-70R, the permeate Au_x-70P was concentrated and diafiltered with 15 × 20 mL of water with a 50 kDa diafiltration membrane. The retentate $Au_{2.6}$-50R was collected, and the permeate Au_x-50P was concentrated and diafiltered with 15 × 20 mL of water with a 30 kDa diafiltration membrane. The retentate $Au_{2.5}$-30R was collected, and the permeate Au_x-30P was concentrated on a 10 kDa diafiltration membrane, yielding $Au_{2.0}$-10R. TEM images and UV−vis spectra were collected for samples Au_x-10R to 70R.

III. Results and Discussion

Sufficient purification of nanoparticle samples can often be more challenging than the preparation itself, involving tedious, time-consuming, and wasteful procedures such as extensive solvent washes and fractional crystallization. Yet obtaining gold nanoparticle samples that are free of impurities such as free ligand, precursor molecules, salts, and undesired nanoparticles is necessary for many applications. In this section, we describe the results of studies aimed at evaluating the efficacy of diafiltration for (i) removal of small molecule impurities from gold nanoparticles, (ii) separation of a bimodal population of nanoparticles into the corresponding small and large fractions, and (iii) the fractionation of a polydisperse nanoparticle sample.

Traditional Methods of Purification. Purification of the 2-[2-(2-mercaptoethoxy)ethoxy]ethanol 3-nm particles is typically achieved by precipitation in hexane followed by diethyl ether and ethyl acetate washes and finally ultracentrifugation twice at 60 000 rpm.[20] However, some impurities often remain after such treatments. Due to our interest in the properties and self-assembly of ligand-stabilized nanoparticles, we sought purification schemes that would yield higher purity nanoparticles in a more efficient fashion. As a first approach, we carried out a rigorous combination of extraction with CH_2Cl_2, Sephadex chromatography, and ultracentrifugation, each of which is considered a standard purification technique. A second approach, dialysis, has also been employed for purification. Dialysis is advantageous due to the fact that purification can be carried out with water alone. Despite an improvement in purity over the literature method,[20] these two approaches had some drawbacks that needed to be addressed: (1) Extractions are not generally applicable for the removal of free ligand, especially when the solubilities of the ligand and ligand-stabilized particle are similar. Additionally, while we have reduced the volume of organic solvent used, a more toxic halogenated solvent has been employed. (2) The 3-nm nanoparticles tend to irreversibly bind to the Sephadex chromatography support, decreasing the yield and limiting reuse of the chromatographic material. (3) Ultracentrifugation can be difficult or impractical on larger scales and requires a significant time investment, increasing the time required for preparation of nanoparticle samples to 3 days. (4) Dialysis produces a large amount of aqueous waste and requires a significant time investment.

Diafiltration as an Approach to Nanoparticle Purification. To address the drawbacks of the standard purification techniques described above, we investigated a third approach, diafiltration, as a means of preparing pure nanoparticles while reducing solvent dependence, increasing yields, and increasing the efficiency of the purification process. Diafiltration has been commonly used in the biological sciences for a number of applications.[41,42,52,53] Like dialysis, diafiltration membranes are rated by their nominal molecular weight cutoff (MWCO), wherein a 10 kDa membrane will retain 90% of a globular protein with a molecular mass >10 kDa.[54] In the case of nanoparticles, the MWCO can be correlated to such nanoparticle properties as core size, ligand shell thickness, and hydrodynamic radius, and to solution properties such as pH and ionic strength. In our studies, we have found that membranes with a MWCO of 10−100 kDa are appropriate for neutral, water-soluble nanoparticles with a core diameter of 1−5 nm.

Unlike other membrane filtration techniques, such as dialysis or stirred-cell ultrafiltration, diafiltration (Figure 1) is considered a continuous flow process, wherein the sample to be purified or separated is continually passed over the membrane surface. While traditional ultrafiltration can be hindered by the buildup of material on the membrane surface, the continuous flow and constant volume of diafiltration aid in the decreased incidence of membrane fouling. As compared to dialysis, wherein filtration occurs via passive means, hydrostatic pressure as a result of continuous flow is the driving force behind diafiltration. Additionally, each diafilter contains a number of membrane surfaces, greatly enhancing the surface area available for filtration. Due to the continuous flow and high surface area of this technique, diafiltration allows for very efficient and rapid purification and size separation.[54,55]

Diafiltration versus Conventional Methods for Nanoparticle Purification. To compare the effectiveness of diafiltration

(52) Stoner, M. R.; Fischer, N.; Nixon, L.; Buckel, S.; Benke, M.; Austin, F.; Randolph, T. W.; Kendrick, B. S. *J. Pharm. Sci.* **2004**, *93*, 2332−2342.
(53) Shao, J. H.; Zydney, A. L. *Biotechnol. Bioeng.* **2004**, *87*, 286−292.
(54) Cheryan, M. *Ultrafiltration Handbook*; Technomic: Lancaster, PA, 1986.
(55) Brock, T. D. *Membrane Filtration: A User's Guide and Reference Manual*; Science Tech, Inc.: Madison, WI, 1983.

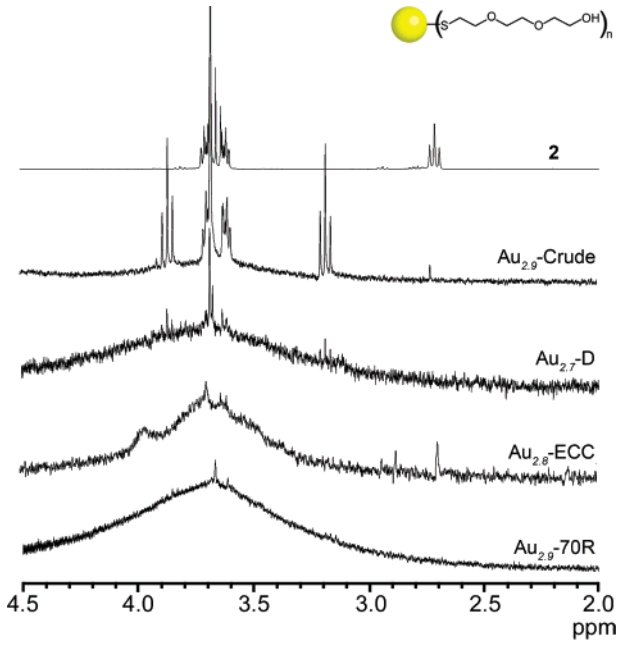

Figure 2. ^{1}H NMR spectra of ligand **2**, crude nanoparticles ($Au_{2.9}$-crude), dialyzed nanoparticles ($Au_{2.7}$-D), nanoparticles purified via extraction, chromatography, and centrifugation ($Au_{2.8}$-ECC), and nanoparticles purified via diafiltration ($Au_{2.9}$-70R). Fine structure in the conventionally purified samples indicates free thiol or disulfide. The absence of fine structure in the diafiltered sample indicates a concentration of free ligand and disulfide below the detection limit of the instrument.

to a conventional purification scheme involving extraction, chromatography, and centrifugation and to dialysis, 3-nm gold nanoparticles passivated with ethylene glycol ligand **2** were purified by one of the three methods and analyzed via NMR, TGA, and XPS.

The amount of organic impurities (thiol and disulfide) in the crude nanoparticles, as well as in the conventionally purified, dialyzed, and diafiltered samples, was assessed via ^{1}H NMR spectroscopy (Figure 2). The spectrum of free ligand **2** shows a triplet at 2.60 ppm, corresponding to the methylene protons α to the thiol, and peaks between 3.46 and 3.62 ppm that correspond to the remaining methylene protons. The spectrum of $Au_{2.9}$-crude exhibits a characteristic broadening of the baseline as is expected for the presence of nanoparticle-bound ligand; however, the sharp signals between 3.20 and 3.92 ppm correspond to a significant amount of free ligand and disulfide in the sample. The NMR spectra of $Au_{2.7}$-D and $Au_{2.8}$-ECC show significantly reduced fine structure, indicating near-complete removal of free ligand; however, some disulfide remains as indicated by the peak at 3.92 ppm. In contrast, the NMR spectrum of $Au_{2.9}$-70R lacks any significant peaks, indicating a free ligand concentration under the NMR detection limit.

The extent of purification by each method was further assessed by XPS and TGA (Table 1). TGA can be used to quantify the percent volatile component in a sample and to distinguish between bound and unbound ligand in a sample based upon differences in the onset time of sample decomposition. A comparison of the total volatile component in $Au_{2.7}$-D (9.9%), $Au_{2.8}$-ECC (13.1%), and $Au_{2.9}$-70R (7.8%) provides strong evidence for greater nanoparticle purity of the diafiltered sample. Calculation of the volatile component based upon a core diameter of 2.9 nm (as determined by TEM) gives ~7.14%, consistent with the TGA data for the diafiltered sample.[19,56] The

Table 1. TGA, XPS, and TEM Results for Different Purification Methods

		XPS (at. %)				
sample	TGA (% vol)	Au 4f	S 2p	Na 1s	Cl 2p	TEM (d_{CORE} nm)
$Au_{2.9}$-crude	10.5[a]	4.1	0.9	38.7	8.4	2.9 ± 1.0
$Au_{2.8}$-ECC	13.1	48.3	6.9	20.6	24.2	2.8 ± 1.0
$Au_{2.7}$-D	9.9	85.8	14.2	*b*	*b*	2.7 ± 0.9
$Au_{2.9}$-70R	7.8	79.8	10.8	4.0	3.3	2.9 ± 0.7

[a] Organic content in $Au_{2.9}$-crude appears low due to the high concentration of salt in the sample, as evidenced in XPS. [b] Concentration below the detection limits.

TGA traces for both the $Au_{2.9}$-crude and $Au_{2.8}$-ECC samples show initial sharp decreases in mass between 120 and 200 °C, followed by a gradual mass loss up to 500 °C. The initial mass loss is likely due to free ligand in the sample, which is easily volatilized at lower temperatures. As the temperature increases beyond 200 °C, nanoparticle-bound ligands desorb and are volatilized. In contrast, the diafiltered sample $Au_{2.9}$-70R shows a continuous decrease in sample mass over the entire TGA trace, with the greatest change in mass occurring once the temperature reaches 200 °C. These results strongly indicate that the diafiltered sample contains no free ligand.

We further employed quantitative XPS analysis as a method for determining the relative atomic percentage of Au, S, Na, and Cl in each sample, allowing for the measurement of both free and bound ligand as well as salts in the sample. The $Au_{2.9}$-crude, $Au_{2.8}$-ECC, $Au_{2.7}$-D, and $Au_{2.9}$-70R samples exhibit Au:S ratios of 4.6:1, 7.0:1, 6.1:1, and 7.4:1, respectively, further demonstrating that $Au_{2.9}$-70R has the lowest concentration of free thiol. The atomic percentage of both Na and Cl is also reduced in $Au_{2.9}$-70R compared to $Au_{2.8}$-ECC and within experimental error of $Au_{2.7}$-D, demonstrating the ability of diafiltration to remove not only free ligand but also excess salt in the samples.

Analysis of the NMR, TGA, and XPS data clearly demonstrates that diafiltration allows for the preparation of nanoparticle samples with a higher degree of purity than is available by conventional means, showing in all cases impurity concentrations below that of conventionally prepared samples. This high degree of purity made possible by diafiltration has recently been exploited in the preparation of 1D and 2D self-assembled structures.[14,15] Our comparison further shows that aqueous diafiltration is more convenient, efficient, and green than conventional purification, allowing for the removal of free ligand and excess salts in a single purification step. In addition, diafiltration is more rapid, allowing for complete purification in as little as 15 min compared with up to 3 days for conventional approaches to purification. Thus, diafiltration offers a much more attractive route to the preparation of high-purity nanoparticles than is available by any previously reported method.

Size Separation of 1.5- and 3-nm Nanoparticles. In addition to its utility for purifications, we found that diafiltration also reduces the polydispersity of as-synthesized nanoparticle samples. When a 70 kDa diafiltration membrane was used for the purification of 3-nm nanoparticles, a fraction (as much as 50%) of the nanoparticles passed through the membrane. TEM analysis of the resultant nanoparticles showed a decreased

(56) Calculations assume complete monolayer coverage, a spherical particle, and a thiol footprint of 0.214 nm^2.

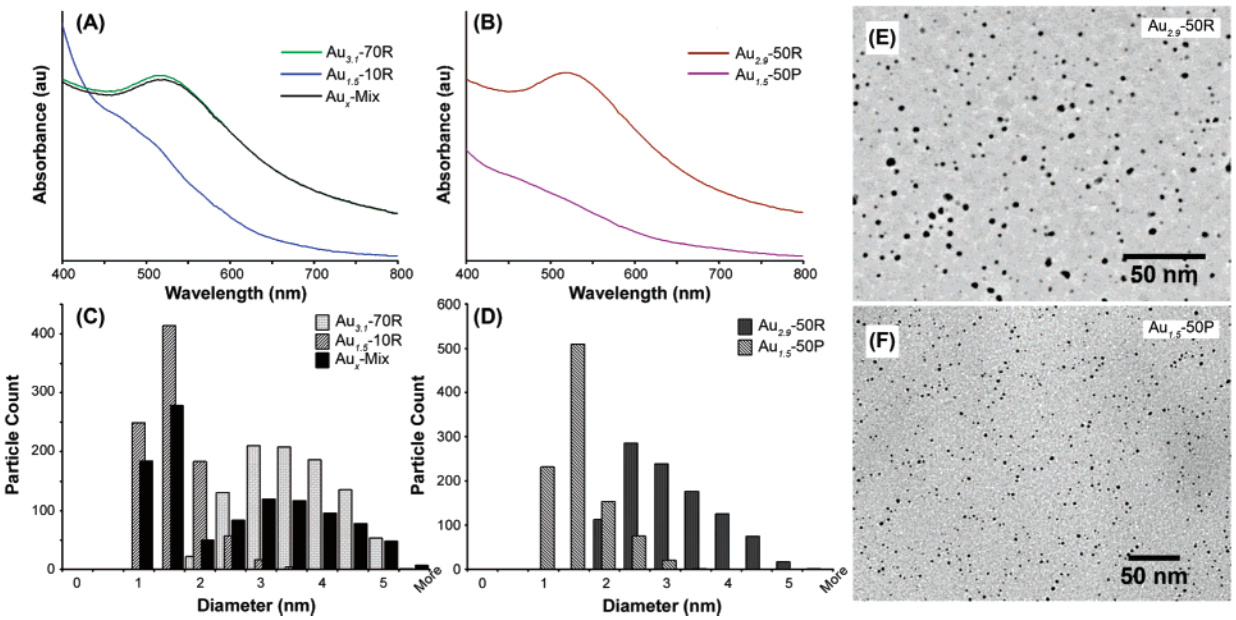

Figure 3. (A) UV−vis spectra for the initial samples $Au_{3.1}$-70R and $Au_{1.5}$-10R and the mixture Au_x-mix. (B) UV−vis spectra of the separated fractions $Au_{2.9}$-50R and $Au_{1.5}$-50P. (C) Stacked TEM histograms for the initial samples $Au_{3.1}$-70R and $Au_{1.5}$-10R and mixture Au_x-mix. (D) Stacked TEM histograms for the separated fractions $Au_{2.9}$-50R and $Au_{1.5}$-50P. (E, F) Representative TEM images of the separated fractions $Au_{2.9}$-50R and $Au_{1.5}$-50P.

polydispersity over nanoparticles purified by conventional methods (Table 1). On the basis of these results, we explored the possibility of using diafiltration for the deliberate separation of nanoparticle samples.

As an initial experiment, we investigated the separation of a bimodal mixture of nanoparticles (Au_x-mix) prepared from purified 1.5- and 3.1-nm nanoparticles. A 1:1 molar mixture of $Au_{1.5}$-10R and $Au_{3.1}$-70R was prepared and diafiltered with 15 × 10 mL of water with a 50 kDa diafiltration membrane. Following diafiltration, the permeate and retentate fractions were analyzed via TEM and UV−vis, and the data were compared to those for $Au_{3.1}$-70R, $Au_{1.5}$-10R, and Au_x-mix.

We used the intensity, peak width, and peak location (λ_{max}) of the plasmon peak in the UV−vis spectra as an indicator of the core size of each sample (Figure 3A,B). The initial 3.1-nm sample ($Au_{3.1}$-70R) exhibits the characteristic plasmon resonance expected for a nanoparticle with a large core diameter.[57] In contrast, $Au_{1.5}$-10R lacks a plasmon peak, indicative of sub-2-nm gold particles (Figure 3A). The spectrum of Au_x-mix is similar to that of the initial 3.1-nm sample but with a slightly broadened plasmon peak due to the presence of an equivalent of 1.5-nm particles, as expected for a more polydisperse sample.[57] Following separation of the mixture by diafiltration, the UV−vis spectrum of the retentate $Au_{2.9}$-50R exhibits the plasmon absorption expected for large nanoparticles (Figure 3B). The permeate shows no plasmon peak in the UV−vis spectrum, consistent with the smaller core size of the particles that have been eluted during diafiltration.

The successful separation of the bimodal nanoparticle mixture suggested by UV−vis spectroscopy was confirmed by TEM analysis of the core sizes (Figure 3C−F). Figure 3C shows the size distributions for the initial 1.5- and 3.1-nm samples and the mixed sample, which has the expected bimodal distribution. Following diafiltration, the histograms of $Au_{2.9}$-50R and $Au_{1.5}$-50P are unimodal (Figure 3D) with core diameters of 2.9 ± 1.0 and 1.5 ± 0.5 nm, showing successful separation into fractions similar to the initial nanoparticle samples. The slight decrease in core size of the retentate in comparison to the initial 3.1-nm sample is due to some fraction of larger particles from the 1.5-nm sample being retained. Given the initial overlap of the particle distributions, minor changes in the mean core size and distribution are expected.

The performance of the diafiltration approach for this type of size separation is remarkable due to the high resolution of the separation and because it can be carried out in water on the benchtop with simple equipment. The ease of this separation as well as the versatility afforded in the separation of water-soluble materials with as little as 1.5 nm size difference will make diafiltration an invaluable tool in a number of applications, from synthesis and catalysis to assessing the biological impacts of nanoparticles.

Fractionation of Nanoparticles. On the basis of the performance observed in our original separation experiment, we attempted to use diafiltration for the fractionation of a polydisperse gold nanoparticle sample. Because standard nanoparticle preparations yield nanoparticles with polydispersity of up to 30%, the ability to fractionate samples into several monodisperse fractions would be very valuable. For example, by removal of the upper and lower edges of a size distribution, samples approaching monodispersity could be envisaged.

Figure 4 outlines the fractionation of a polydisperse nanoparticle sample by multiple diafiltration steps. In the first step, the crude nanoparticles are diafiltered for 15 volumes with a 70 kDa diafiltration membrane to remove the largest fraction of nanoparticles and aggregates, yielding $Au_{2.9}$-70R. The process is repeated, each time concentrating and diafiltering the permeate of the previous step with a smaller MWCO membrane (i.e., 50 kDa, 30 kDa). The final diafiltration step with a 10 kDa diafiltration membrane serves as a purification of the smallest core size fraction.

(57) Link, S.; El-Sayed, M. A. *Int. Rev. Phys. Chem.* **2000**, *19*, 409−453.

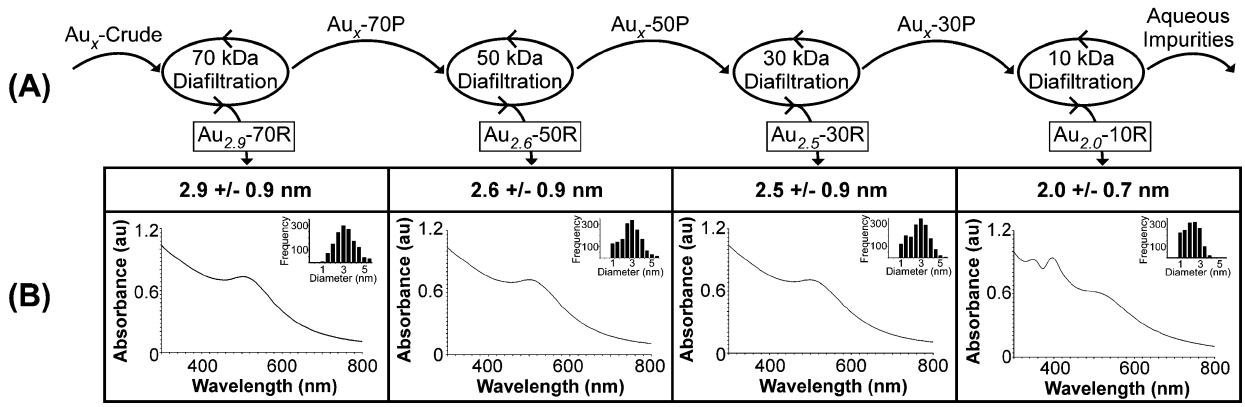

Figure 4. (A) Diafiltration scheme used for obtaining nanoparticle fractions.[58] Following each diafiltration step, the retentate is analyzed via UV-vis and TEM and the permeate is further diafiltered on a smaller MWCO membrane. (B) Summary UV-vis and TEM data for each fraction. With each decrease in pore size, the average core size decreases, with corresponding blue shifts and broadening of the plasmon resonance peak in the UV-vis spectrum.

Size separation can be observed visually through a change in color for each fraction, with the 70 kDa fraction having a distinct purple hue characteristic of large gold nanoparticles and the 10 kDa fraction having the brown color of smaller gold nanoparticles. Normalized UV−vis spectra for each of the diafiltered fractions are shown in Figure 4B and in Supporting Information Figure S5. The spectrum of the 70 kDa fraction exhibits the most pronounced plasmon peak with a λ_{max} of 527 nm. The 50 kDa spectrum has a λ_{max} of 522 nm, whereas λ_{max} has shifted to 521 nm for the 30 kDa fraction, and both have broadened, indicating that the average core size decreases from the 70 kDa fraction to the 30 kDa fraction. The largest change in the plasmon peak can be seen for the 10 kDa fraction, which is significantly broadened, indicating a smaller mean core size; additional peaks at 350 and 410 nm suggest the presence of nanoparticles of ~1-nm diameter.[59,60]

We further evaluated the core diameter and size distribution for each fraction via TEM analysis (Figure 4, Supporting Information Figure S6). In agreement with the UV−vis data, the 70 kDa retentate fraction exhibits the largest core size with an average core diameter of 2.9 ± 0.9 nm. As the MWCO of the membranes decreases, the average core diameters also decrease to 2.6 ± 0.9 and 2.5 ± 0.9 nm for the 50 kDa and 30 kDa retentate samples, respectively. The 10 kDa retentate fraction displays the greatest decrease in core size and polydispersity, with an average diameter of 2.0 ± 0.7 nm.

While we have shown that the separation of 1.5- and 3-nm nanoparticles is possible with diafiltration, the results of the fractionation reveal the lower limits of diafiltration's ability. Though a decrease in average core diameter is observed, the size dispersity of the fractions is higher than desired when commercial diafiltration membranes are used. Two main factors contribute to the polydispersity of the samples. First, irregularities in the membrane pores lead to an increase in the passage of nanoparticles into the permeate that are larger than expected for a given MWCO. Second, the similar size of the nanoparticles and the membrane pores leads to a lower rate of small particle removal per volume (increased σ).[61] A further consequence of the similar size is membrane fouling due to the occlusion of nanoparticles within the membrane pores decreasing separation efficiency. Electrostatic repulsion or attraction between charged particles and the membrane surface can similarly affect σ or lead to membrane fouling. Though diafiltration remains a promising approach for convenient nanoparticle fractionation there is a clear need for the development of membranes with appropriate material and pore characteristics for preparing monodisperse nanoparticle fractions.

IV. Conclusion

In this article we have demonstrated that diafiltration is capable of efficient and convenient purification and size separation. Our experiments have shown that diafiltration is particularly well suited for the purification of aqueous nanoparticle samples, removing all detectable organic impurities and salts, and surpassing the purity achievable via conventional means. Diafiltration is an efficient, rapid, and versatile purification method, allowing for the complete purification of any small, water-soluble nanoparticle in as little as 15 min. In addition to using a more benign solvent (water) and reducing the volume of organic solvents used in the nanoparticle preparation, the diafiltration membranes are fairly inexpensive for routine use and can be reused with proper care, making diafiltration a greener purification scheme than the other methods discussed. The higher purity afforded by diafiltration will allow for more precise determination of electronic and optical properties, easier assessment of structure−function relationships in toxicology studies, and greater reproducibility in the self-assembly of nanoparticles. Additionally, the ability to separate small molecules from nanoparticles should allow for the assessment of catalytic activity and the isolation of catalysis products from nanoparticles.

Our results have also demonstrated that diafiltration is capable of separating 1.5- and 3-nm nanoparticles. Though the σ values for this separation are larger than for purification, leading to some polydispersity, diafiltration remains more efficient and convenient than other reported techniques for the separation of similar samples. The ability to quickly size-separate samples is a powerful tool and can be exploited to separate a wide number

(58) Fractions observed are those that passed through a diafiltration membrane but were retained by the next lower MWCO membrane. For example, Au$_{2.6}$-50R is the permeate of the 70 kDa diafiltration but the retentate of the 50 kDa diafiltration.

(59) Schaaf, T. G.; Shafigullin, M. N.; Khoury, J. T.; Vezmar, I.; Whetten, R. L.; Cullen, W. G.; First, P. N.; Gutierrez-Wing, C.; Ascensio, J.; Jose-Yacaman, M. J. *J. Phys. Chem B* **1997**, *101*, 7885−7891.

(60) Gutierrez, E.; Powell, R. D.; Furuya, F. R.; Hainfeld, J. F.; Schaaf, T. G.; Shafigullin, M. N.; Stephens, P. W.; Whetten, R. L. *Eur. Phys. J. D* **1999**, *9*, 647−651.

(61) See the Experimental Section.

of nanoscaled materials, allowing for access to and the characterization of materials never before isolated. For example, heterogeneous 3D structures formed from the self-assembly of semiconducting and metal nanoparticles could be separated from individual nanoparticle monomers. Other possible applications include the separation of excess nanoparticles from biological substrates or the separation of seed particles from nanorods, cubes, or prisms.

We expect that these results will establish diafiltration as a convenient and powerful tool for the preparation of pure nanoparticle samples in a simple, efficient, scalable,[45] and green fashion and will allow for convenient access to a wide variety of nanoscaled materials.

Acknowledgment. We thank Stephen Golledge for help with XPS measurements. This research was supported by the National Science Foundation (DUE-0088986).

Supporting Information Available: TGA and UV−vis data as well as additional TEM images/analysis (PDF). This material is available free of charge via the Internet at http://pubs.acs.org.

JA0558241